第二十届全国中高能核物理大会
上海嘉定，2025年4月26日

Study nucleus structure through spectator particle yield in relativistic heavy-ion collisions

Jun Xu (徐骏)

Tongji University

Main collaborators: Lu-Meng Liu(刘鹿蒙)(Fudan)、Song-Jie -Li(李松桀)(Tongji)
Hai-Cheng Wang(王海澄)(Tongji)、 Chun-Jian Zhang(张春健)(Fudan)
Jiangyong Jia(贾江涌)(Stony Brook)、Zhong-Zhou Ren(任中洲)(Tongji)
Guang-Xiong Peng(彭光雄)(UCAS)、Xu-Guang Huang(黄旭光)(Fudan)

Lu-Meng Liu, Chun-Jian Zhang, Jia Zhou, JX*, Jiangyong Jia*, and Guang-Xiong Peng, Phys. Lett. B 834, 137441 (2022), arXiv: 2203.09924 [nucl-th]

Lu-Meng Liu, Chun-Jian Zhang, JX*, Jiangyong Jia*, and Guang-Xiong Peng, Phys. Rev. C 106, 034913 (2022), arXiv: 2209.03106 [nucl-th]

Lu-Meng Liu, JX*, and Guang-Xiong Peng, Phys. Lett. B 838, 137701 (2023), arXiv: 2301.07893 [nucl-th]

Probing configuration of α clusters with spectator particles in relativistic heavy-ion collisions
Lu-Meng Liu, Song-Jie Li, Zhen Wang, JX*, Zhong-Zhou Ren*, and Xu-Guang Huang, Phys. Lett. B 854, 138724 (2024), arXiv: 2312.13572 [nucl-th]

Directly probing existence of α-cluster structure in ^{20}Ne by relativistic heavy-ion collisions
Lu-Meng Liu, Hai-Cheng Wang, Song-Jie Li, Chun-Jian Zhang, JX*, Zhong-Zhou Ren*, Jiangyong Jia*, and Xu-Guang Huang*, Phys. Rev. C 111, L021901 (2025), arXiv: 2502.08057 [nucl-th]

Content

- **Probe nucleus structure**
  - **Neutron-skin thickness Δr_{np}~L, $\Delta r_{np}(\theta)$~W_0**
  - **α-cluster structure**
- **Model setup**
  - **Initial density distribution**
  - **Glauber model**
  - **Multifragmentation process**

Neutron skin and E_{sym}

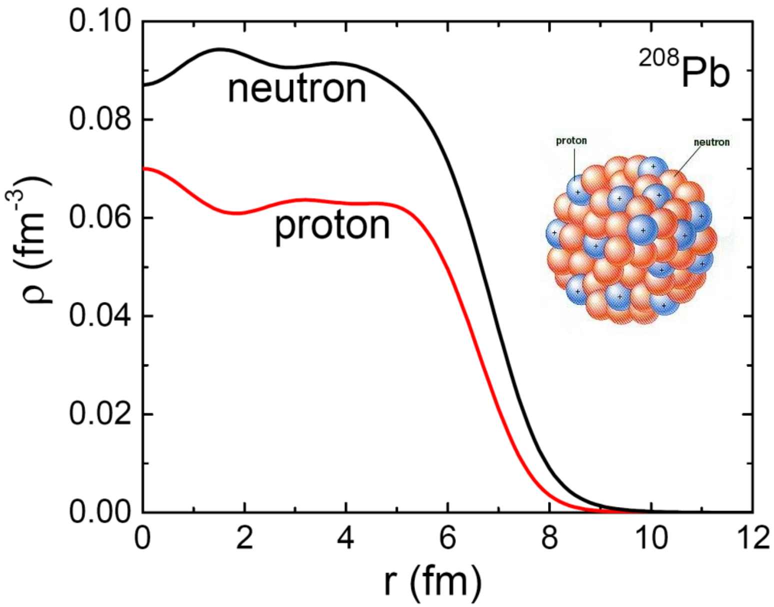

Neutron-Skin Thickness:

$$\Delta r_{np} = \sqrt{\langle r_n^2 \rangle} - \sqrt{\langle r_p^2 \rangle} \quad \text{(fm)}$$

For ^{208}Pb:

$\Delta r_{np} = 0.211^{+0.054}_{-0.063}$ fm **from proton scattering**

$\Delta r_{np} = 0.16 \pm 0.07$ fm **from pion scattering**

$\Delta r_{np} = 0.18 \pm 0.04(\text{expt.}) \pm 0.05(\text{theor.})$ fm **from $\bar{p}$ annihilation**

$\Delta r_{np} = 0.15 \pm 0.03(\text{stat.})^{+0.01}_{-0.03}(\text{sys.})$ fm **from coherent pion photoproduction**

$\Delta r_{np} = 0.283 \pm 0.071$ fm **from parity-violating electron scatterings**

Energy per nucleon in asymmetric matter

Symmetry energy

$$E(\rho,\delta) \approx E_0(\rho) + \boxed{E_{sym}(\rho)}\,\delta^2$$

Energy per nucleon in symmetric matter

$\rho=\rho_n+\rho_p$

$\delta=(\rho_n-\rho_p)/\rho$

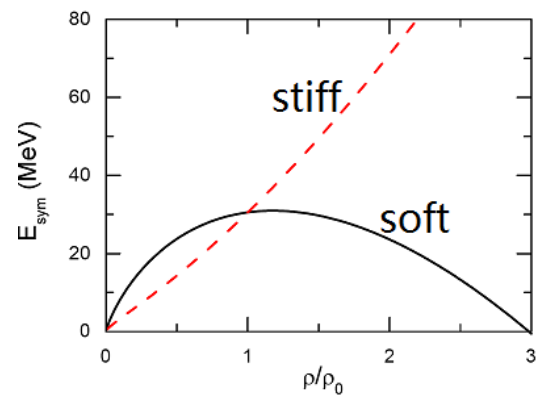

Expansion around saturation density ρ_0

$$E_{sym}(\rho) = E_{sym}(\rho_0) + L\chi + \ldots$$

$$\chi = \frac{\rho-\rho_0}{3\rho_0}$$

Slope parameter

$$L = 3\rho_0 \left[\frac{\partial E_{sym}(\rho)}{\partial \rho}\right]_{\rho=\rho_0}$$

Various constraints on $E_{sym}(\rho_0)$ and $L(\rho_0)$

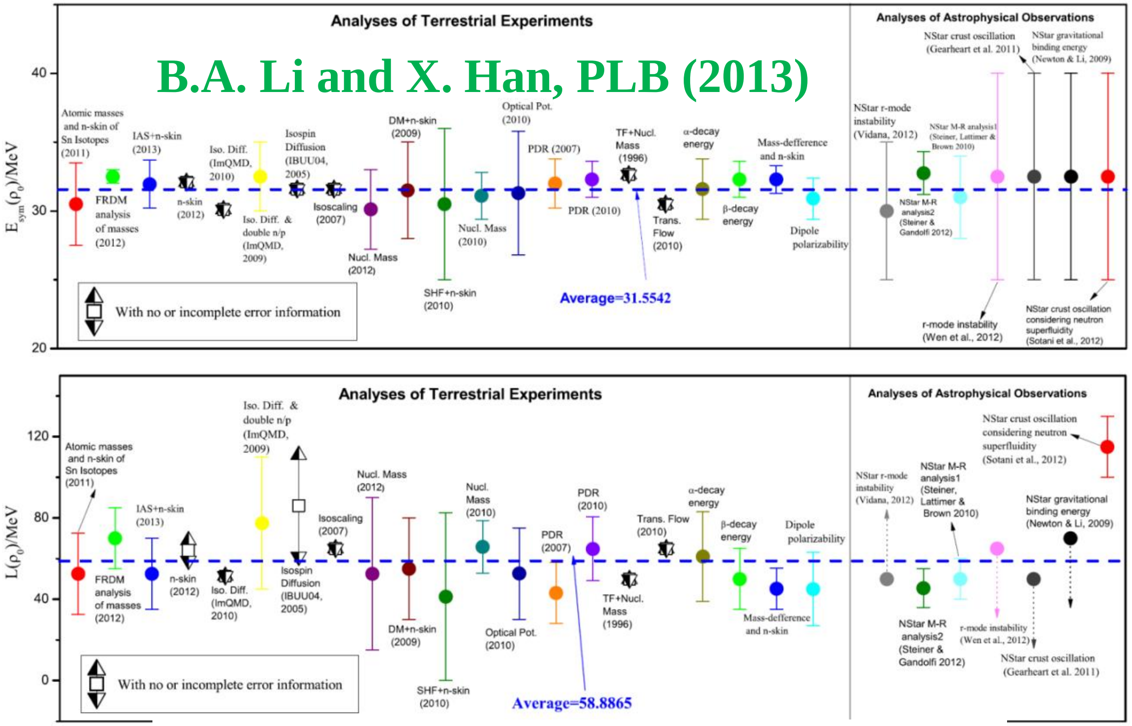

B.A. Li and X. Han, PLB (2013)

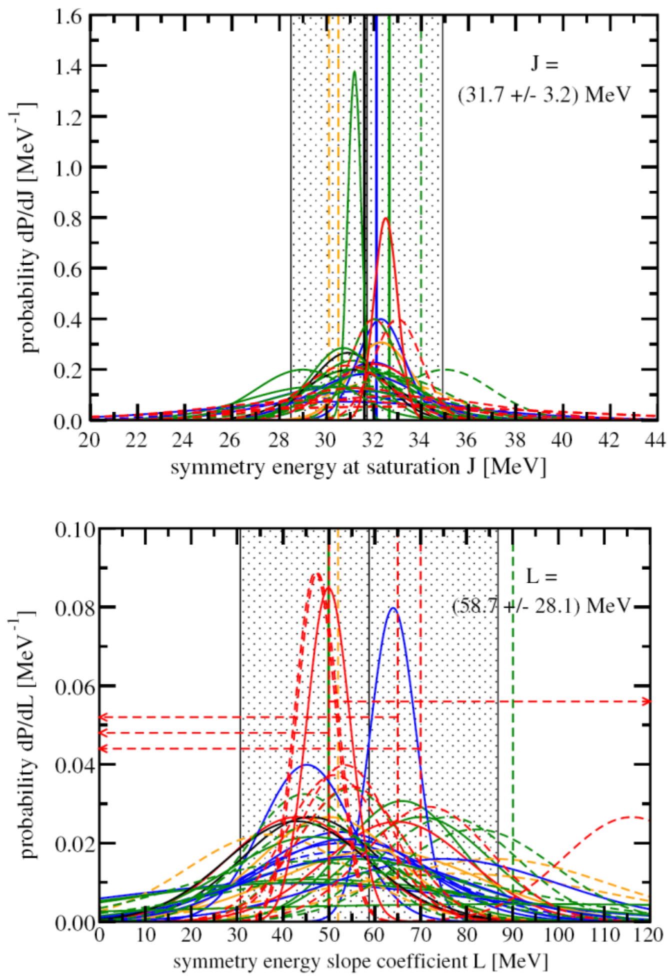

M. Oertel et al., RMP (2017)

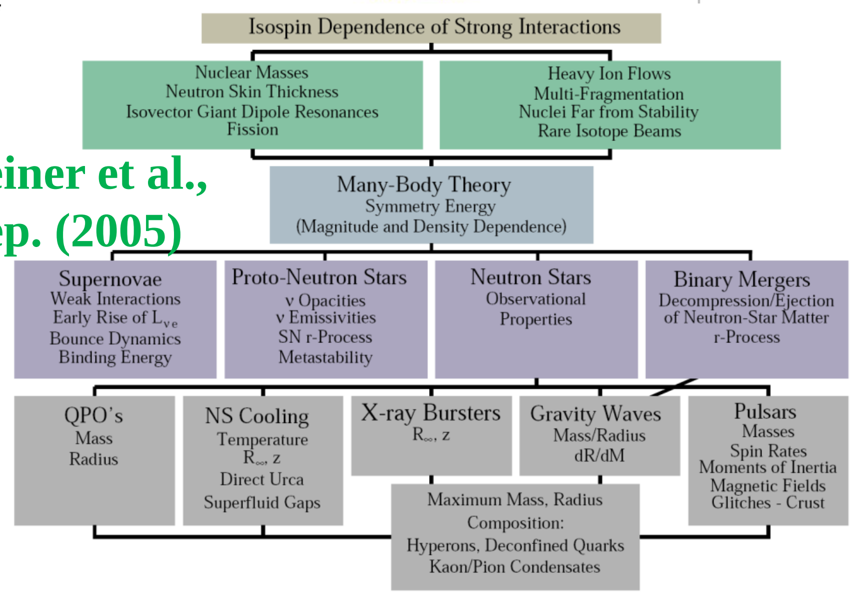

A.W. Steiner et al., Phys. Rep. (2005)

Symmetry energy PACS: 21.65.Ef

More reliable probes are still needed

probe neutron skin with mid-rapidity observables at RHIC and LHC

Charged-particle multiplicity

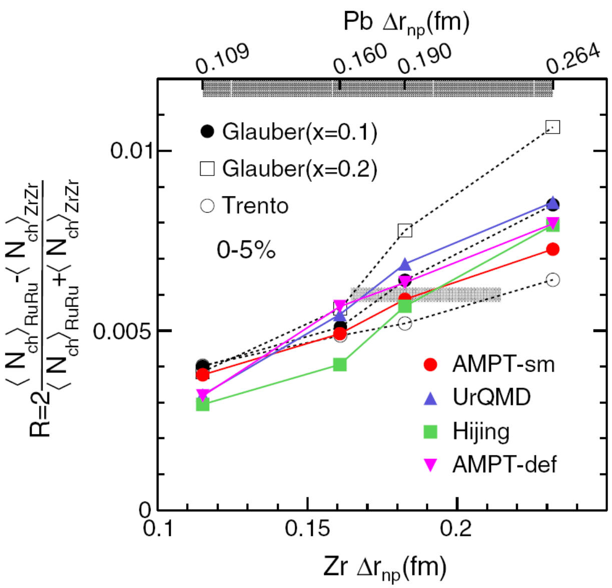

H.L. Li et al., PRL (2020)

v_2 and $<p_T>$

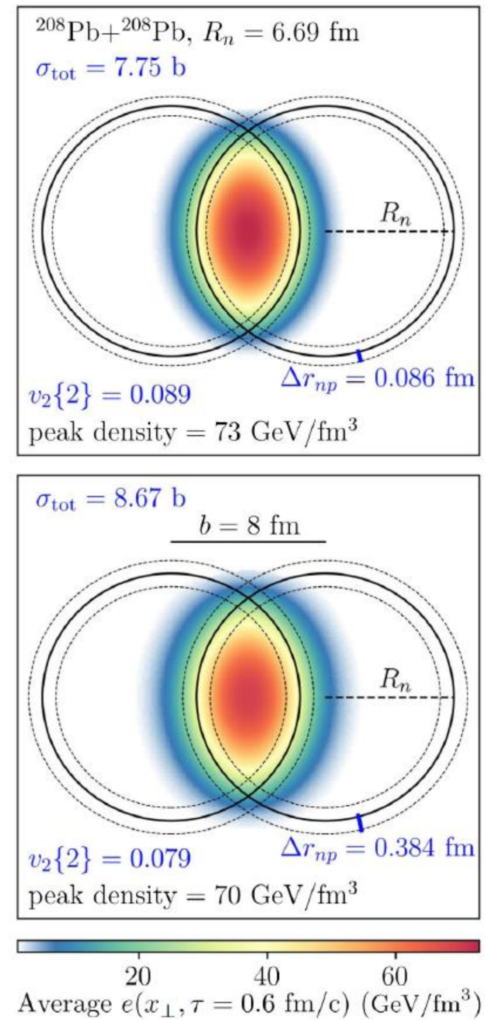

G. Giacalone, G. Nijs, and W. van der Schee, PRL (2023)

probe the density distribution of colliding nuclei

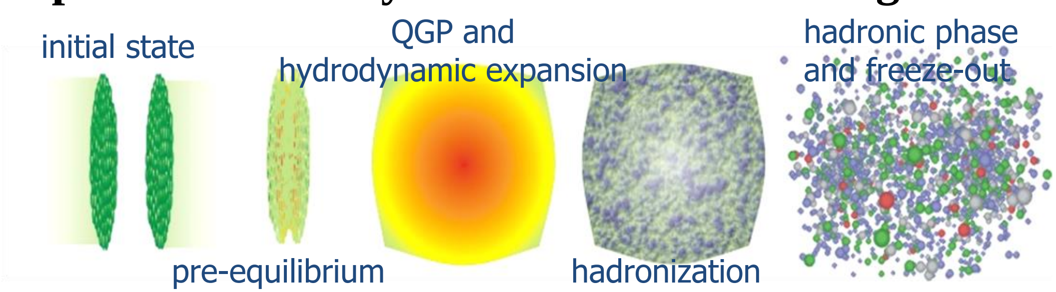

Observables at midrapidities suffer from complicated dynamics and model dependence

probe neutron skin with intermediate-energy HIC

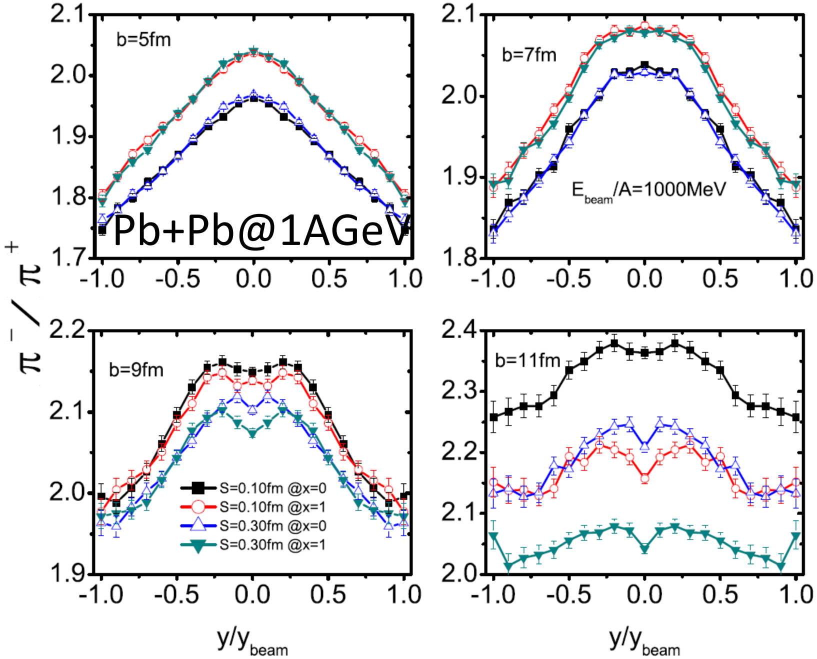

G.F. Wei et al., PRC (2014)

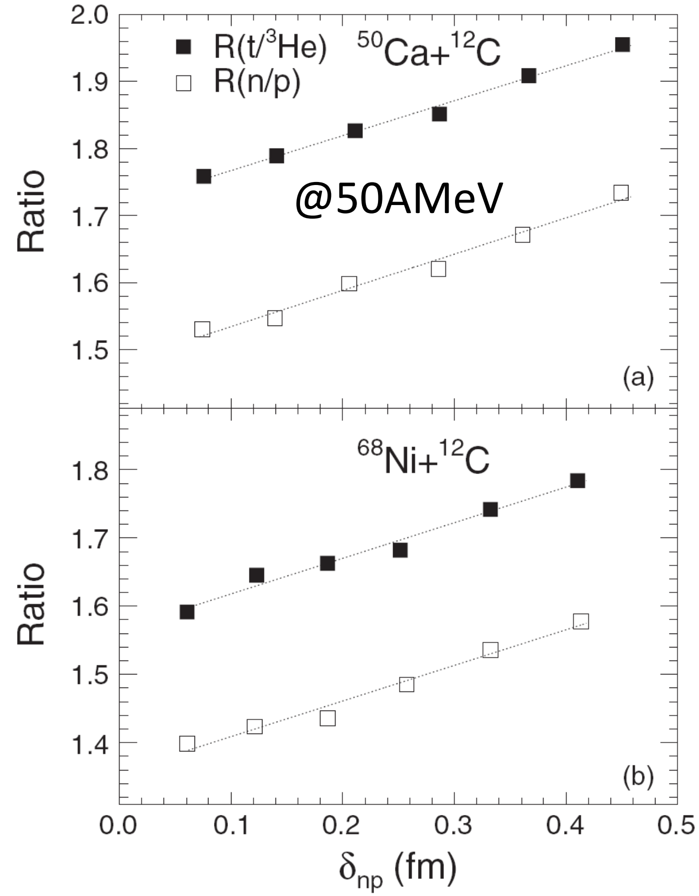

Z.T. Dai et al., PRC (2014)

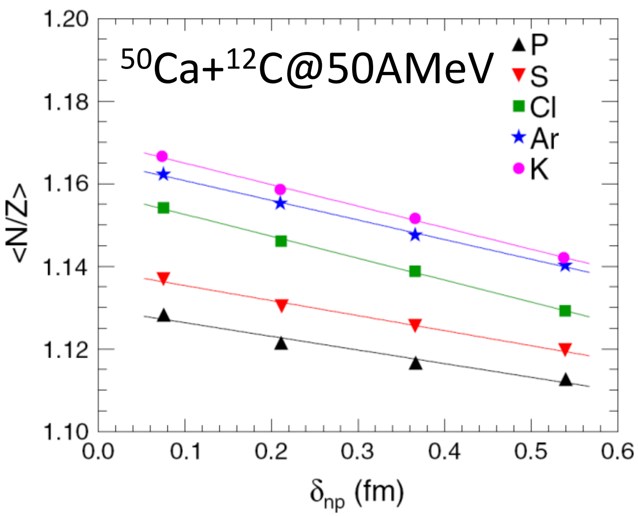

Z.T. Dai et al., PRC (2015)

Suffer from:

1) Model dependence
2) Interaction between spectator and participant
3) Uncertainties of clusterization/multifragmentation

Basic idea of our studies

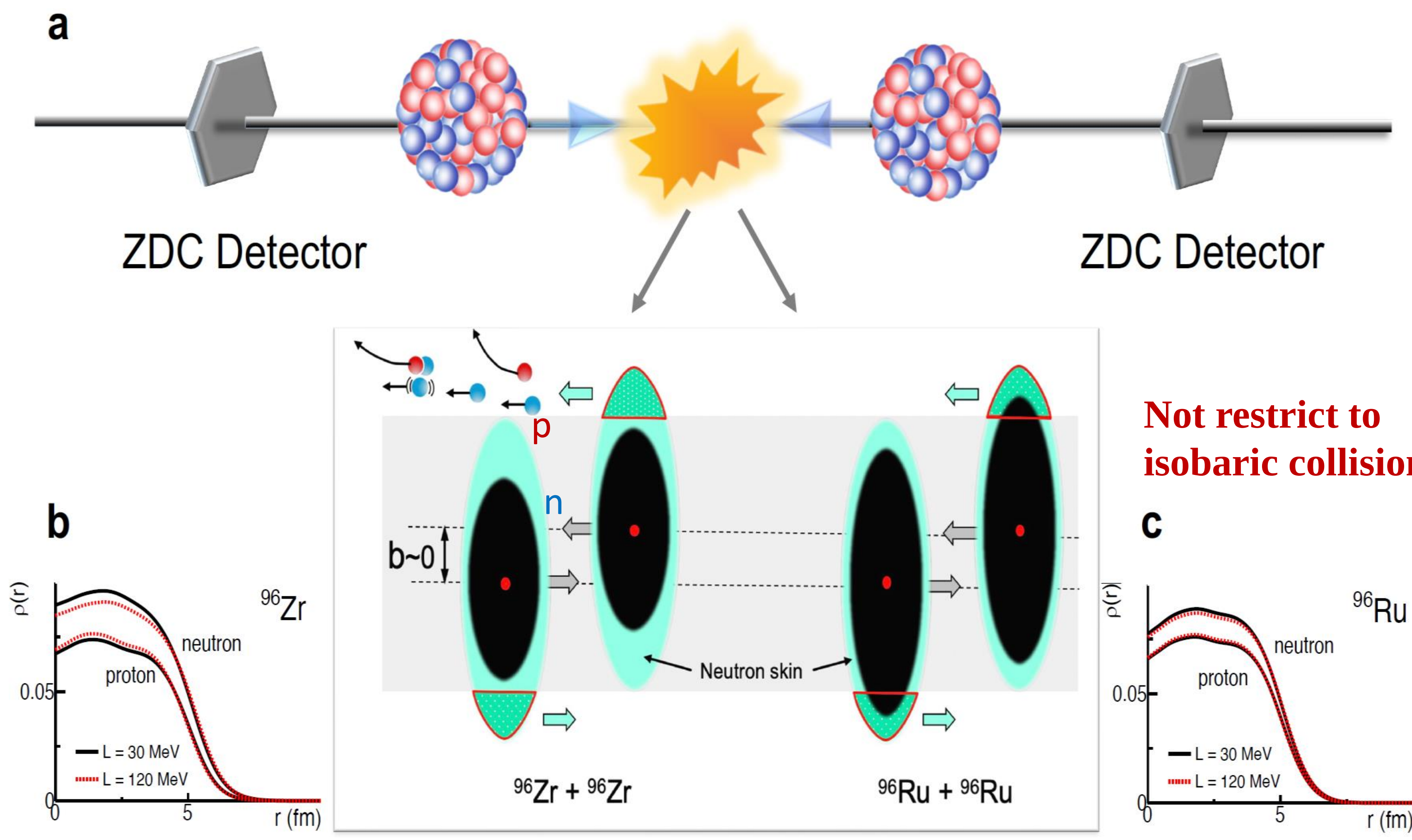

Not restrict to isobaric collisions

Advantages:

1) **Spectator matter has almost no interaction with participant matter**
2) **UCC region, free from uncertainties of clusterization/multifragmentation**

Model setup: initial density distribution

Skyrme-Hartree-Fock (SHF) model:

$$\begin{aligned} v(\vec{r}_1, \vec{r}_2) &= t_0(1 + x_0 P_\sigma)\delta(\vec{r}) \\ &+ \frac{1}{2}t_1(1 + x_1 P_\sigma)[\vec{k}'^2\delta(\vec{r}) + \delta(\vec{r})\vec{k}^2] \\ &+ t_2(1 + x_2 P_\sigma)\vec{k}' \cdot \delta(\vec{r})\vec{k} \\ &+ \frac{1}{6}t_3(1 + x_3 P_\sigma)\rho^\alpha(\vec{R})\delta(\vec{r}) \\ &+ iW_0(\vec{\sigma}_1 + \vec{\sigma}_2)[\vec{k}' \times \delta(\vec{r})\vec{k}]. \end{aligned}$$

Quantity	MSL0	Quantity	MSL0
t_0 (MeV fm^5)	−2118.06	ρ_0 (fm^{-3})	0.16
t_1 (MeV fm^5)	395.196	E_0 (MeV)	−16.0
t_2 (MeV fm^5)	−63.953 1	K_0 (MeV)	230.0
t_3 (MeV fm$^{3+3\sigma}$)	128 57.7	$m^*_{s,0}/m$	0.80
x_0	−0.070 949 6	$m^*_{v,0}/m$	0.70
x_1	−0.332 282	$E_{\rm sym}(\rho_0)$ (MeV)	30.0
x_2	1.358 30	L (MeV)	60.0
x_3	−0.228 181	G_S (MeV fm^5)	132.0
σ	0.235 879	G_V (MeV fm^5)	5.0
W_0 (MeV fm^5)	133.3	$G_0'(\rho_0)$	0.42

L.W. Chen, C.M. Ko, B.A. Li, and JX PRC (2010)

Pairing interaction

$$V_{\rm pair}^{(n,p)} = V_0^{(n,p)}\left(1 - \frac{1}{2}\frac{\rho(\vec{r})}{\rho_0}\right)\delta(\vec{r}_1 - \vec{r}_2)$$

Hartree-Fock method:

$$E = \sum_i \left\langle i \left| \frac{p^2}{2m} \right| i \right\rangle + \frac{1}{2}\sum_{ij}\langle ij|\,\tilde{v}_{12}\,|ij\rangle$$

$$\frac{\delta}{\delta\phi_i}\left(E - \sum_i e_i \int |\phi_i(\vec{r})|^2 d^3r\right) = 0$$

$$\left[-\vec{\nabla}\cdot\frac{\hbar^2}{2m_q^*(\vec{r})}\vec{\nabla} + U_q(\vec{r}) + \vec{W}_q(\vec{r})\cdot(-i)(\vec{\nabla}\times\vec{\sigma})\right]\phi_i = e_i\phi_i$$

Particle density

$$\rho_q(\vec{r}) = \sum_{i,\sigma} |\,\phi_i(\vec{r},\sigma,q)|^2$$

Hartree-Fock-Bogoliubov method:

$$\int d^3\mathbf{r}' \sum_{\sigma'} \begin{pmatrix} h(\mathbf{r}\sigma, \mathbf{r}'\sigma') & \tilde{h}(\mathbf{r}\sigma, \mathbf{r}'\sigma') \\ \tilde{h}(\mathbf{r}\sigma, \mathbf{r}'\sigma') & -h(\mathbf{r}\sigma, \mathbf{r}'\sigma') \end{pmatrix} \begin{pmatrix} \varphi_1(E, \mathbf{r}'\sigma') \\ \varphi_2(E, \mathbf{r}'\sigma') \end{pmatrix} = \begin{pmatrix} E + \lambda & 0 \\ 0 & E - \lambda \end{pmatrix} \begin{pmatrix} \varphi_1(E, \mathbf{r}\sigma) \\ \varphi_2(E, \mathbf{r}\sigma) \end{pmatrix}$$

Particle density **Pairing density**

$$\rho(r) = \sum_i \varphi_2(E_i, r)^2 \qquad \tilde{\rho}(r) = -\sum_i \varphi_1(E_i, r)\varphi_2(E_i, r)$$

Reproduce E_b and R_c within 1.5%

M.V. Stoitsov et al., CPC (2013)

Model setup: initial density distribution

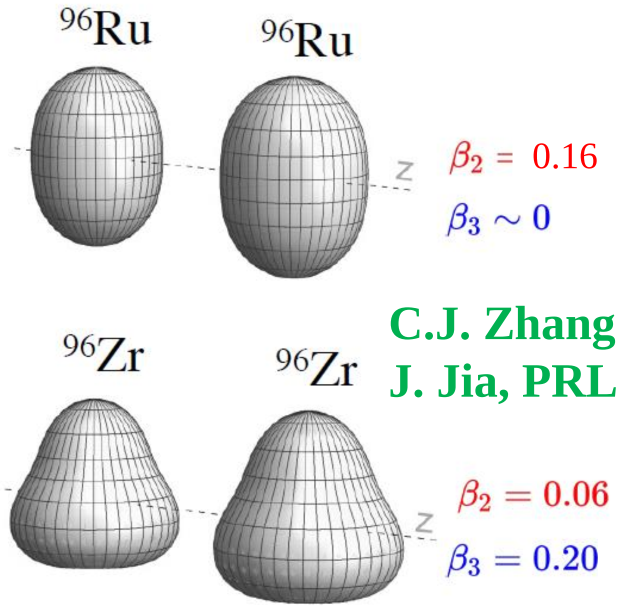

C.J. Zhang and J. Jia, PRL (2022)

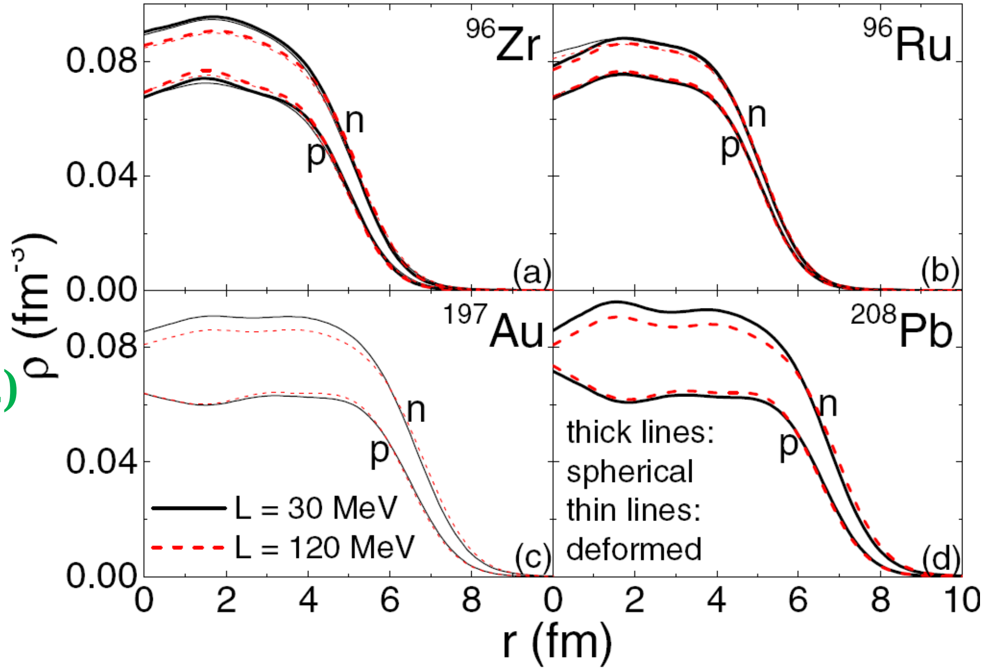

Multipole moments

$$Q_{\lambda,\tau} = \int \rho_\tau(\vec{r}) r^\lambda Y_{\lambda 0}(\theta) d^3 r$$

Deformation parameters

$$\beta_{\lambda,\tau} = \frac{4\pi Q_{\lambda,\tau}}{3 N_\tau R^\lambda}$$

Constrained SHFB calculation with fixed Q_λ (β_λ)

TABLE II. Neutron-skin thicknesses Δr_{np} and deformation parameters β_2 and β_3 for different nuclei using different slope parameters L of the symmetry energy from SHFB calculations.

Nucleus	β_2, β_3	Δr_{np} (fm) $L = 30$ MeV	$L = 120$ MeV
^{96}Zr	0, 0	0.147	0.231
	0.06, 0.2 [43]	0.145	0.227
^{96}Ru	0, 0	0.028	0.061
	0.16, 0 [43]	0.026	0.058
^{197}Au	−0.15, 0 [44,45]	0.127	0.243
^{208}Pb	0, 0	0.149	0.281

Model setup: Glauber model

Schematic Monte-Carlo Glauber model

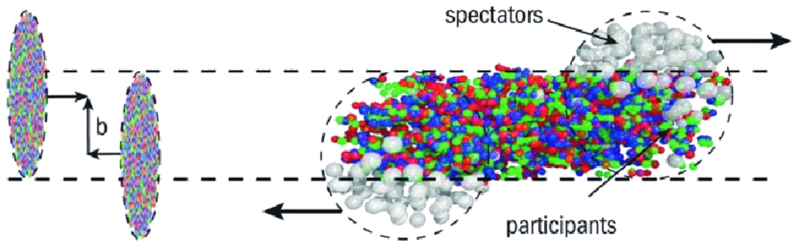

Numbers of sources

$$N_s = (1-x)\frac{N_{\text{part}}}{2} + xN_{\text{coll}}$$

Particle production n from each source

$$p_{\text{nbd}}(n; m, p) = \frac{(n+m-1)!}{(m-1)!n!} p^n (1-p)^m$$

$$p = \frac{\bar{n}}{\bar{n}+m}$$

$\sqrt{s_{NN}}$	130 GeV	200 GeV	5.02 TeV
σ_{NN}	40 mb	42 mb	68 mb

	$\sqrt{s_{\text{NN}}}$	x	$\bar{n}$	m
^{96}Zr + ^{96}Zr	200 GeV	0.12	2.3	2.0
^{96}Ru + ^{96}Ru	200 GeV	0.12	2.3	2.2
^{197}Au + ^{197}Au	130 GeV	0	4.8	4.6
^{197}Au + ^{197}Au	200 GeV	0.10	5.8	2.3
^{208}Pb + ^{208}Pb	5.02 TeV	0.09	10.3	3.2

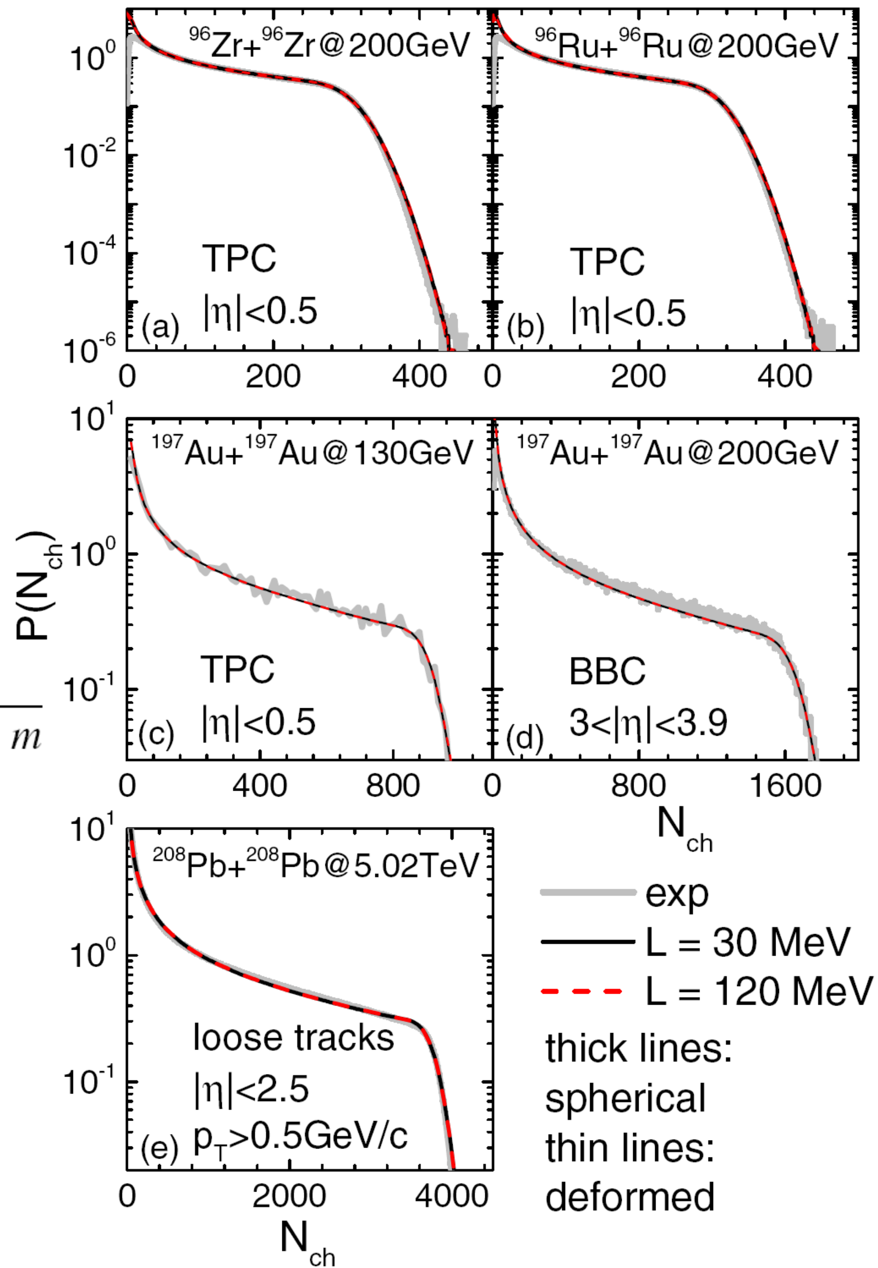

Model setup: multifragmentation process

Dynamics of participant matter is neglected!

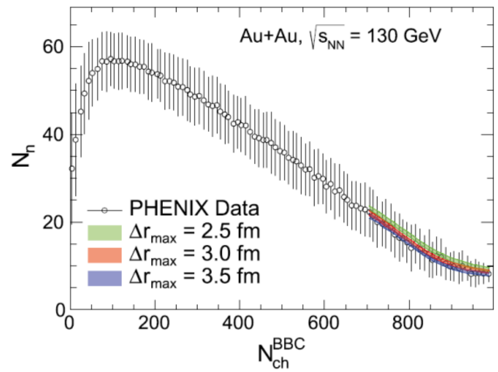

A. Formation of heavy (A>3) clusters

MST
$\Delta r < 3$ fm (empirical nucleon interaction range)
$\Delta p < 300$ MeV/c (empirical Fermi momentum at ρ_0)

B. Heavy (A>3) cluster deexcitation with GEMINI

1. Excitation energy

(test-particle method for parallel events with similar collision configuration)

Simplified SHF EDF

$$
\begin{aligned}
E \;=\; & \frac{1}{N_{TP}}\sum_i\left(\sqrt{m^2+p_i^2}-m\right) \\
& + \int d^3r\left[\frac{a}{2}\left(\frac{\rho}{\rho_0}\right)^2+\frac{b}{\sigma+1}\left(\frac{\rho}{\rho_0}\right)^{\sigma+1}\right] + \int d^3r\left\{\frac{G_S}{2}(\nabla\rho)^2-\frac{G_V}{2}[\nabla(\rho_n-\rho_p)]^2\right\} \\
& + \int d^3r E_{sym}^{pot}\left(\frac{\rho}{\rho_0}\right)^{\gamma}\frac{(\rho_n-\rho_p)^2}{\rho} + \frac{e^2}{2}\int d^3r d^3r' \frac{\rho_p(\vec{r})\rho_p(\vec{r}')}{|\vec{r}-\vec{r}'|} - \frac{3e^2}{4}\int d^3r\left[\frac{3\rho_p}{\pi}\right]^{4/3} - E_{GS}
\end{aligned}
$$

2. Angular momentum

$$\vec{L} = \sum_i \vec{r}_i \times \vec{p}_i$$

Free nucleons:
1) Direct production from A and residue from C
2) Deexcitation from B

C. Coalescence for light (A=2,3) clusters

$$f_d = 8g_d \exp\left(-\frac{\rho^2}{\sigma_d^2} - p_\rho^2\sigma_d^2\right) \qquad f_{t/^3\mathrm{He}} = 8^2 g_{t/^3\mathrm{He}} \exp\left[-\left(\frac{\rho^2+\lambda^2}{\sigma_{t/^3\mathrm{He}}^2}\right) - (p_\rho^2+p_\lambda^2)\sigma_{t/^3\mathrm{He}}^2\right]$$

Results and discussions: spectator particle yield

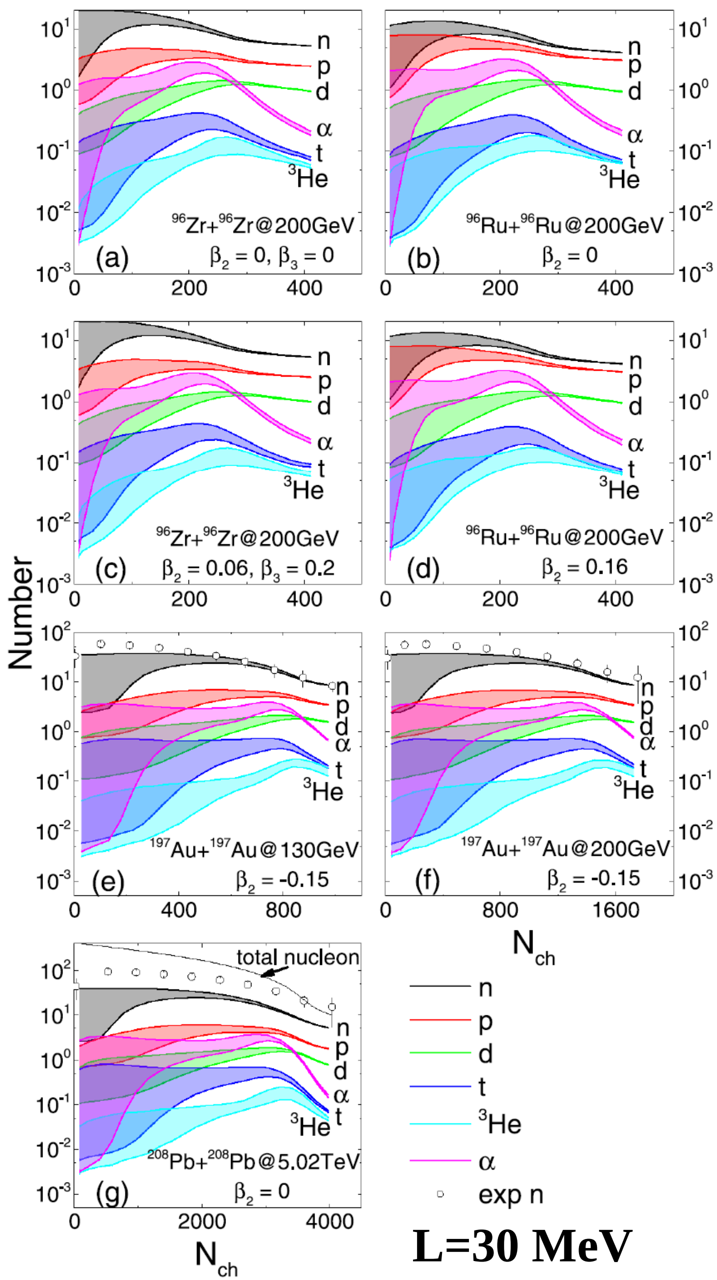

L=30 MeV

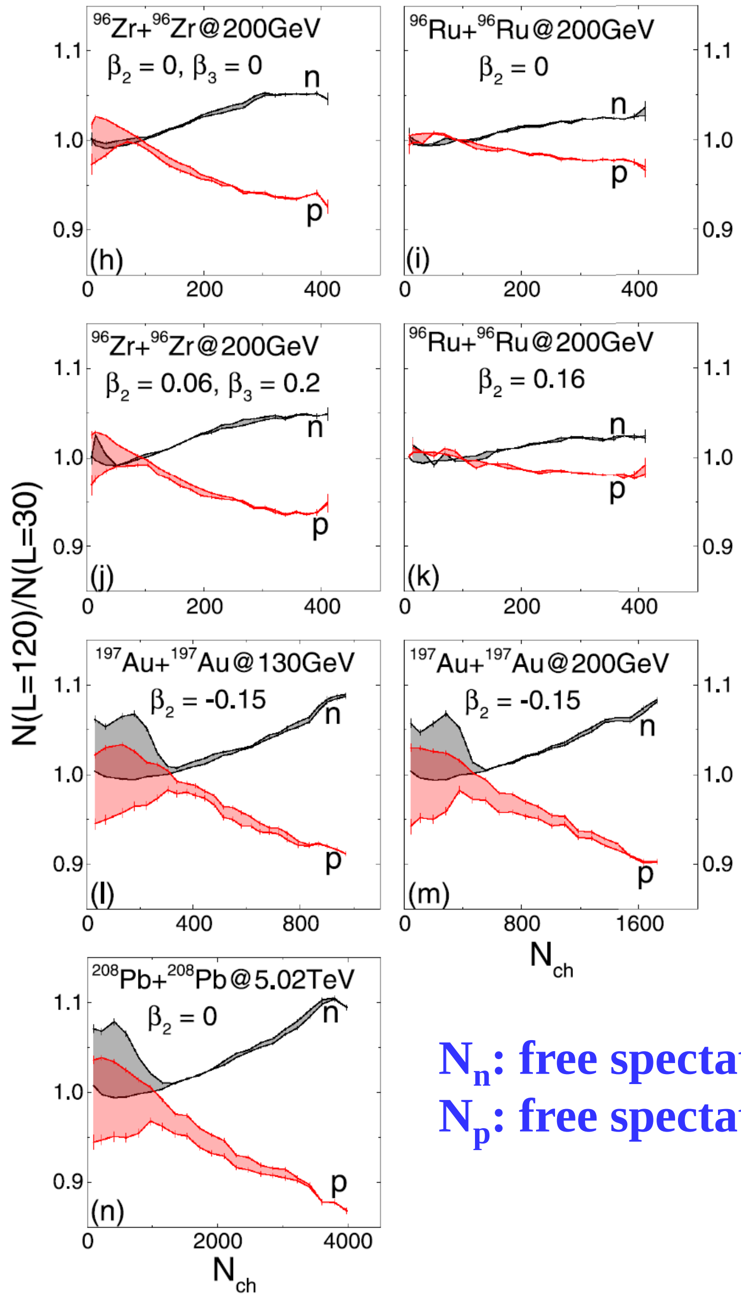

Band:
E/A ±1 MeV

- **Non monitonic dependence on N_{ch}**
- **Difference between N_n and N_p large at UCC, increasing with L or Δr_{np}, with small band**

N_n: free spectator neutron number
N_p: free spectator proton number

Results and discussions: probing L or Δr_{np}

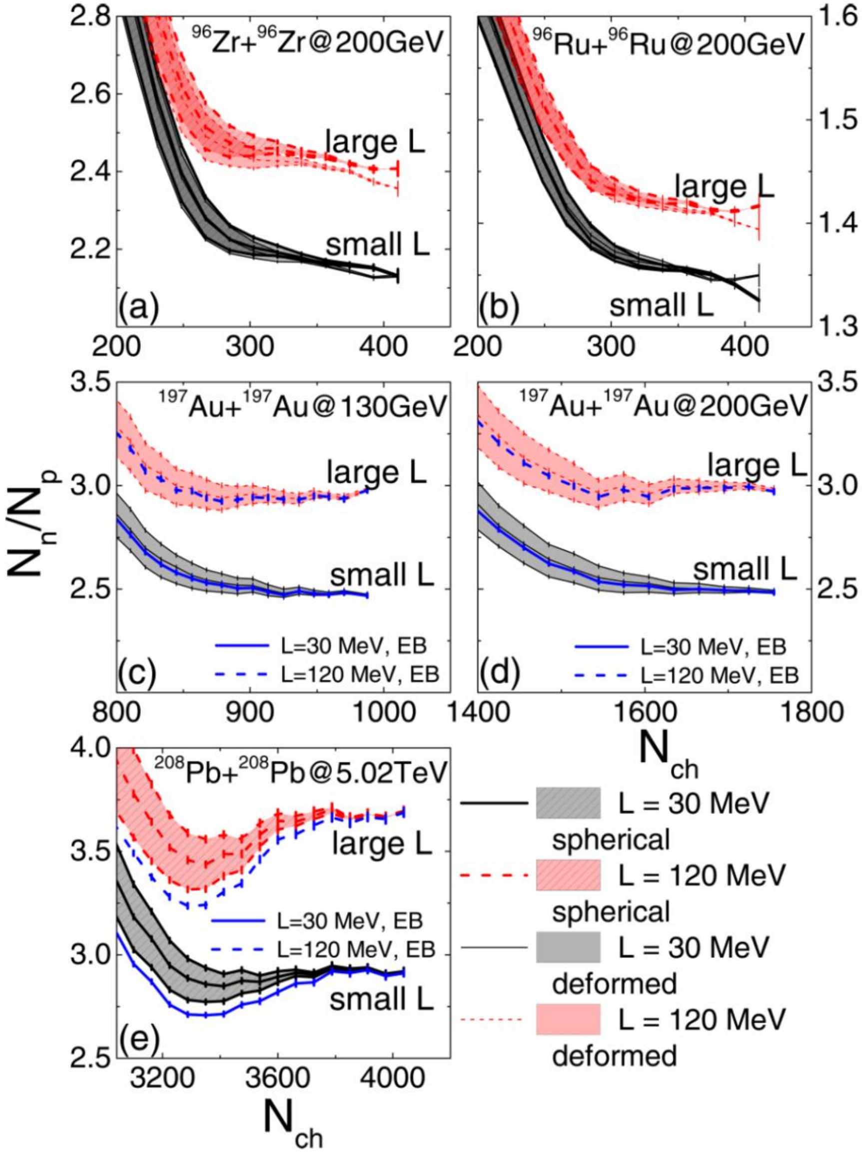

Sn+Sn@40MeV

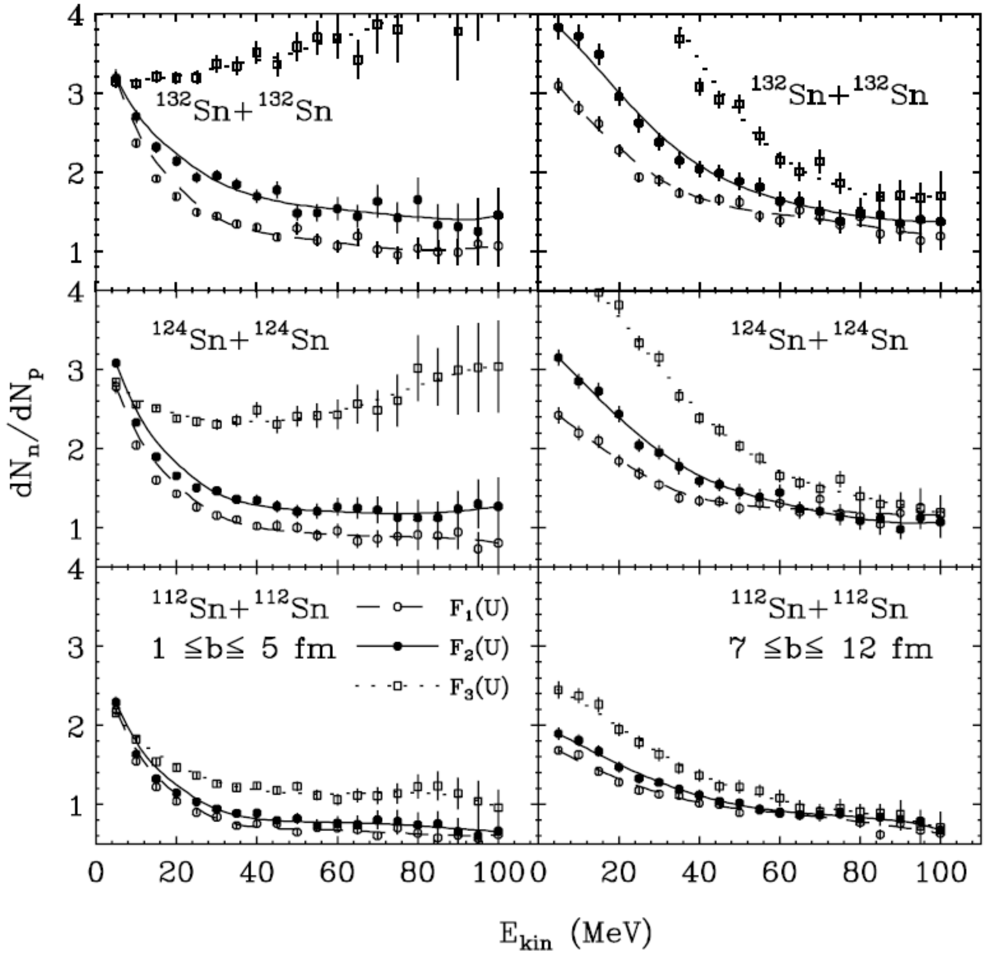

B.A. Li, C.M. Ko, and Z.Z. Ren, PRL (1997)

Results and discussions: probing L or Δr_{np}

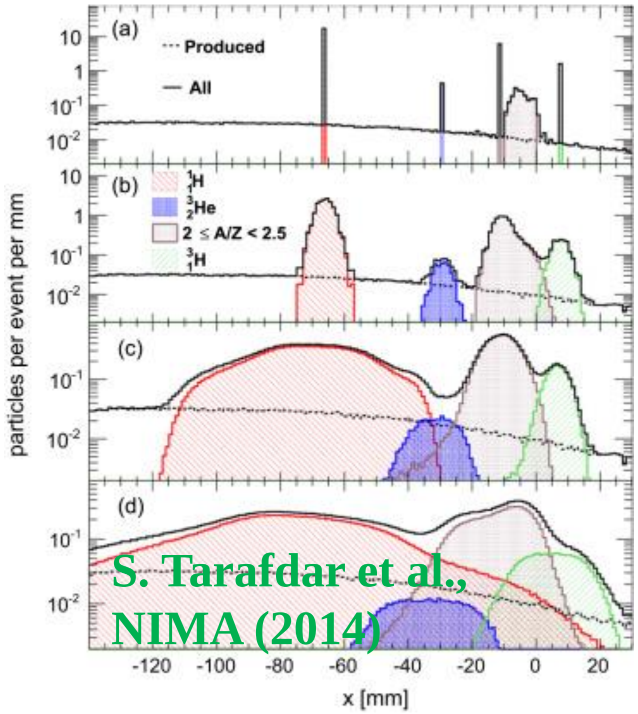

S. Tarafdar et al.,
NIMA (2014)

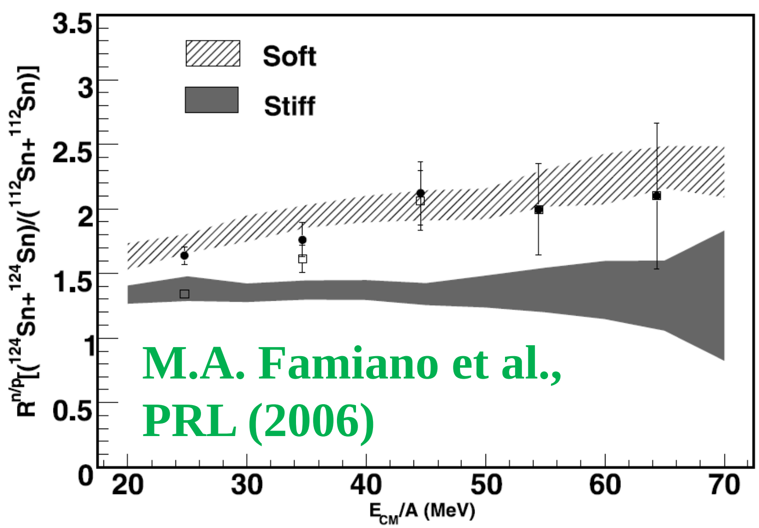

M.A. Famiano et al.,
PRL (2006)

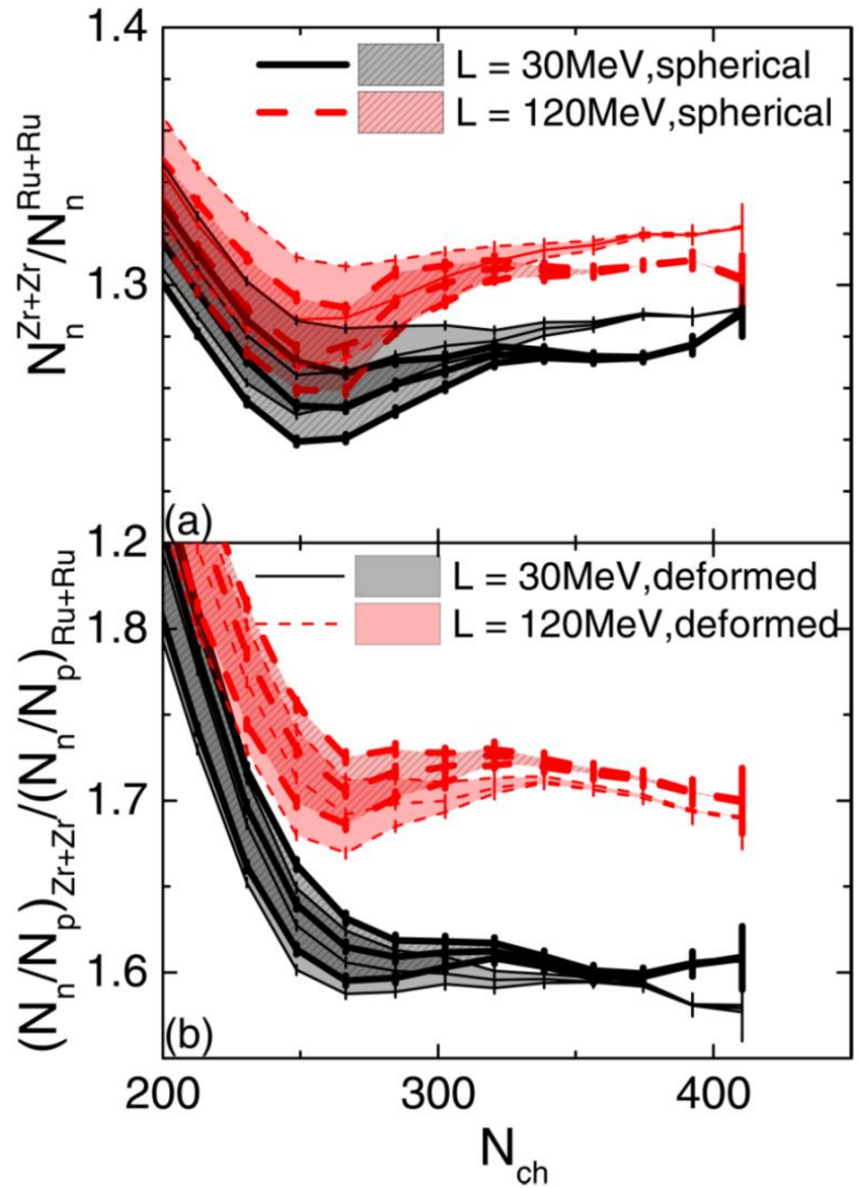

Relevant studies on $\Delta r_{np}(\theta)$ in deformed nuclei

SHF+BCS

Similar Δr_{np} in r and z directions

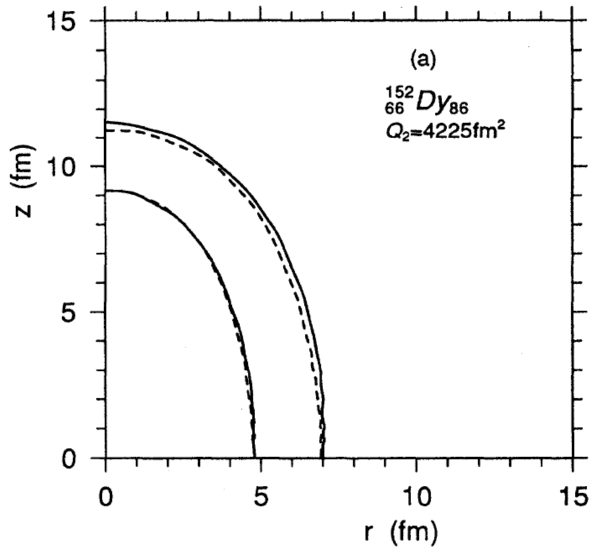

I. Hamamoto and X.Z. Zhang, PRC (1995)

Different Δr_{np} in r and z directions

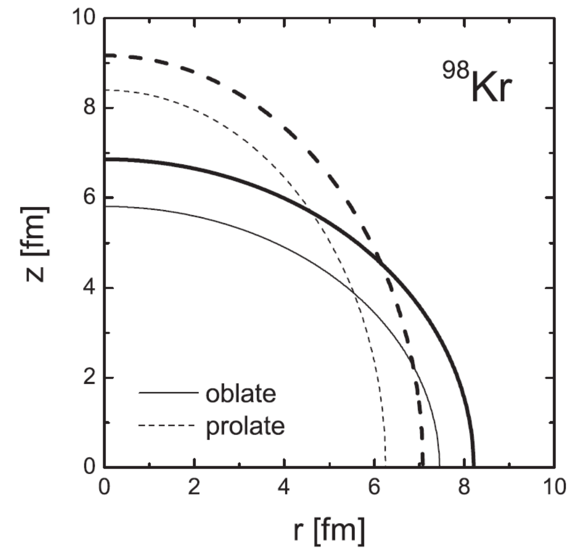

P. Sarriguren et al., PRC (2007)

Affect the scissor-like motion (M1) in deformed nuclei

D. Pena Arteaga and P. Ring, arXiv: 0912.0908 [nucl-th]

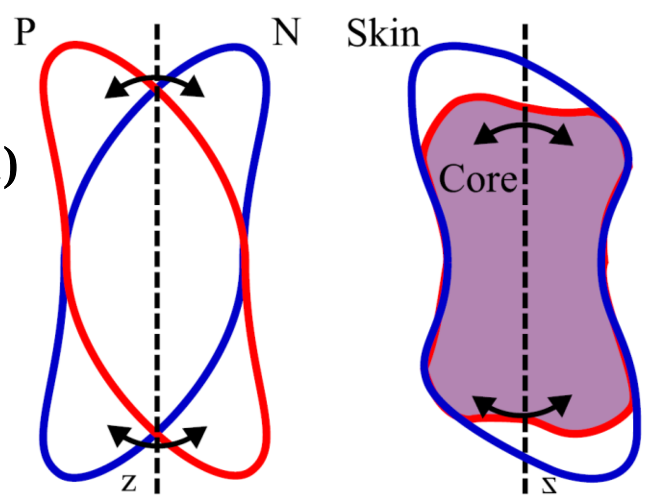

Δr_{np} effect from different collision configurations

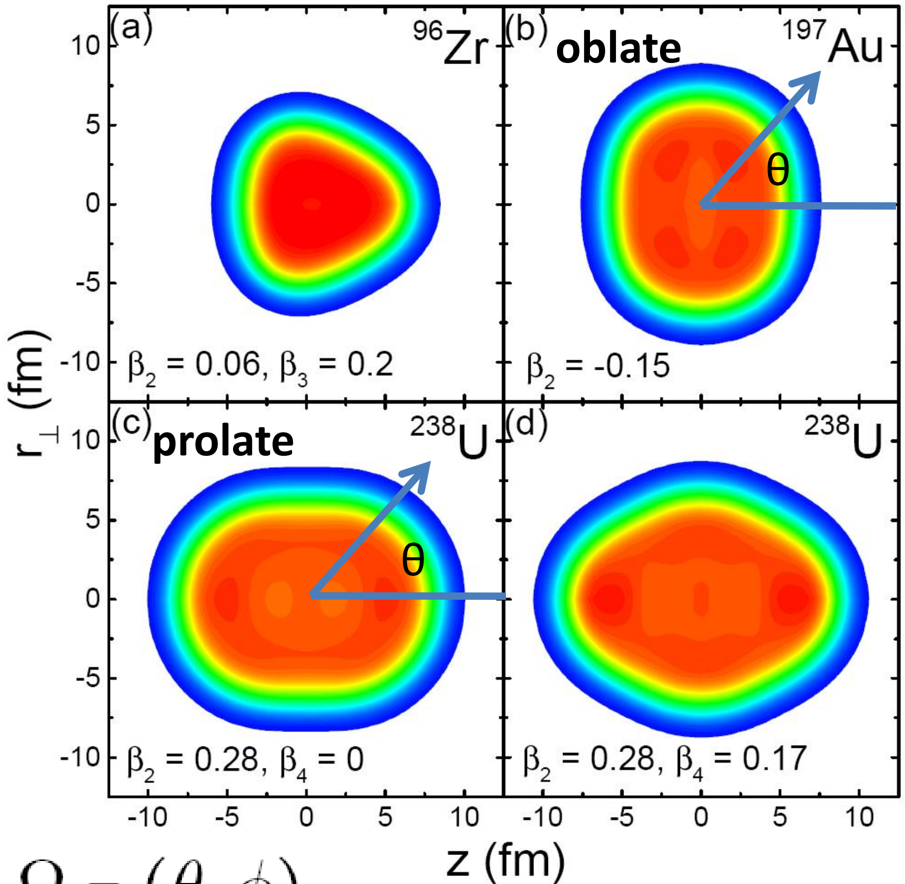

Nucleus	Deformation(s)	$\overline{\Delta r_{np}}$ (fm)	
		L = 30 MeV	L = 120 MeV
^{96}Zr	β_2=0.06, β_3=0.2 [43]	0.145	0.227
^{197}Au	β_2=-0.15 [44]	0.127	0.243
^{238}U	β_2=0.28 [42], β_4=0	0.156	0.291
	β_2=0.28 [42], β_4=0.17	0.153	0.291

Select Δr_{np} at different θ

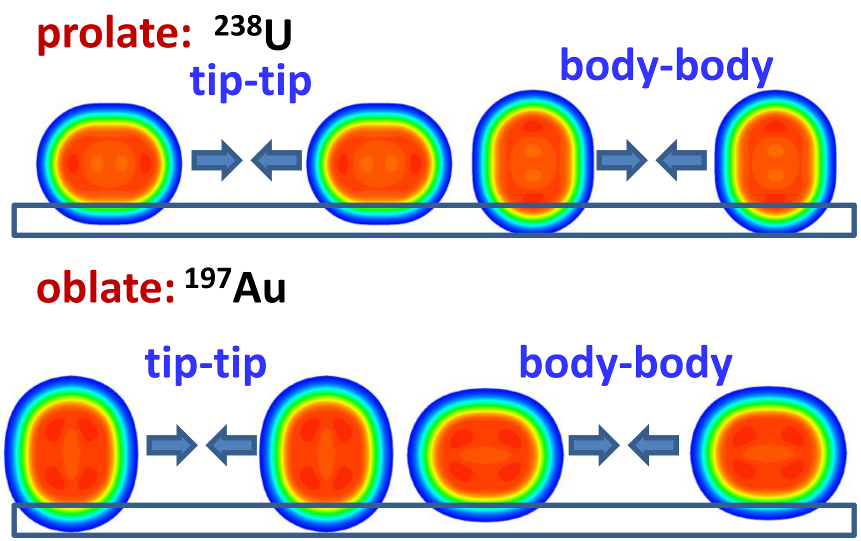

$$\Omega = (\theta, \phi)$$

$$\Delta r_{\rm np}(\Omega) = \sqrt{\langle r_{\rm n}^2(\Omega)\rangle} - \sqrt{\langle r_{\rm p}^2(\Omega)\rangle}$$

$$\sqrt{\langle r_\tau^2(\Omega)\rangle} = \left(\frac{\int \rho_\tau(r,\Omega) r^4 dr}{\int \rho_\tau(r,\Omega) r^2 dr}\right)^{1/2}$$

Deformed Δr_{np} from different SO interactions

SO interaction: affect nucleons in open shells for spin unsaturated nuclei, which contribute to the angular dependence of Δr_{np}

$L \sim U_n - U_p$ has a global effect

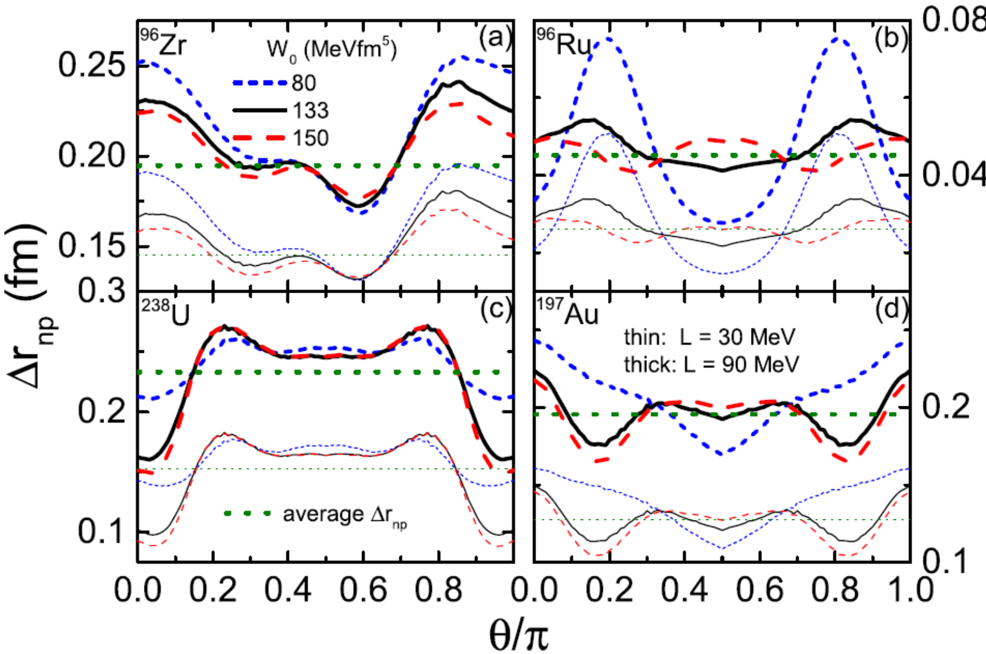

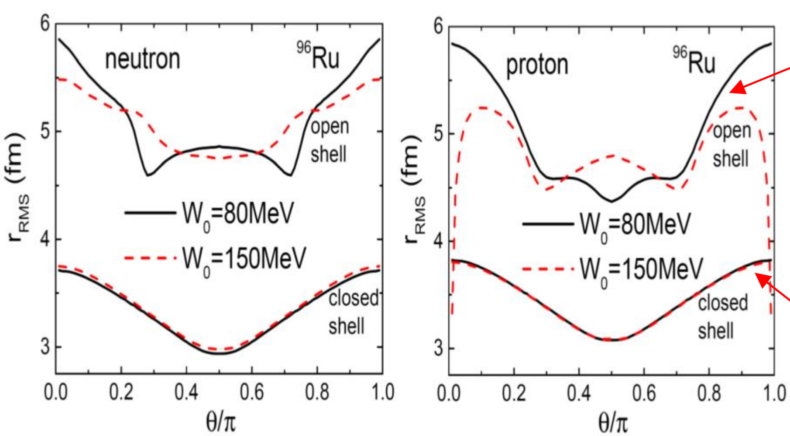

Angular distributions of the RMS radii for typical neutrons (left) and protons (right) in loosely-bound open shells and tightly-bound closed shells of ^{96}Ru using different W_0

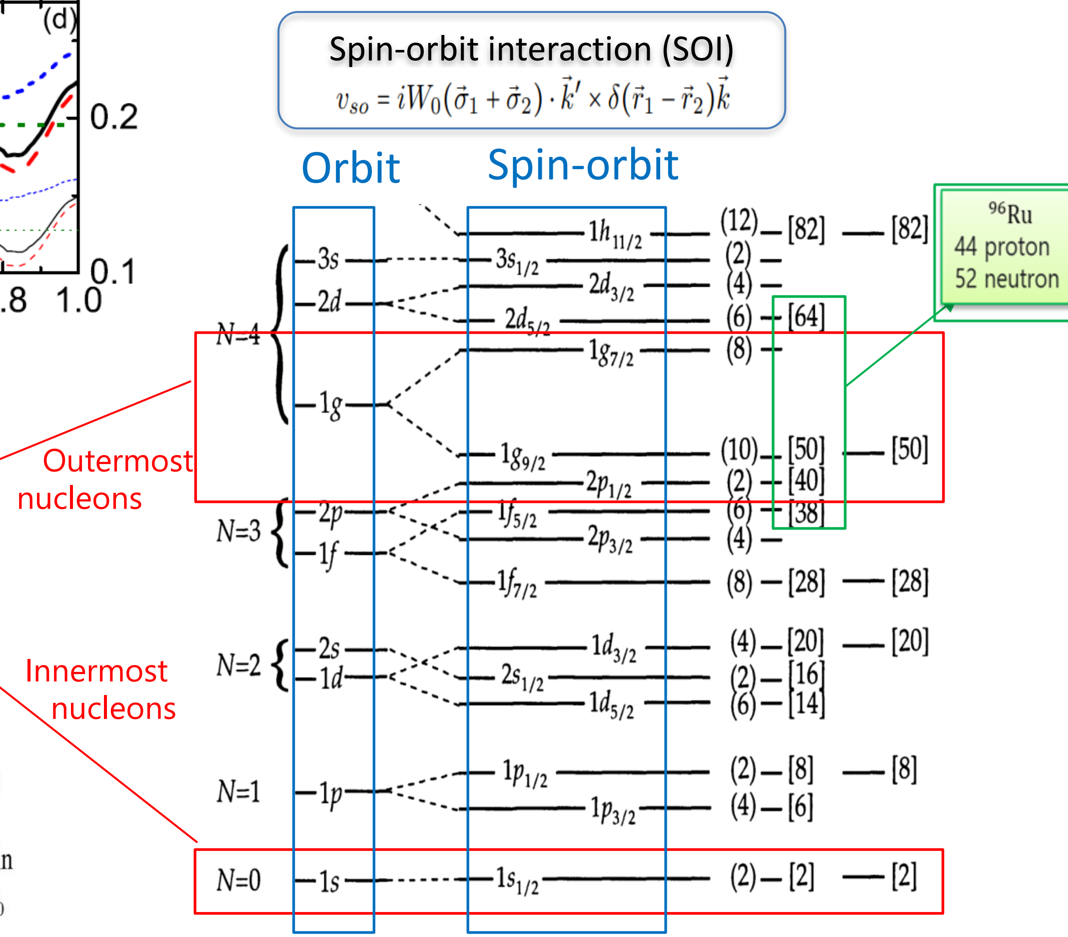

Spectator nucleons from different W_0

b=0 fm

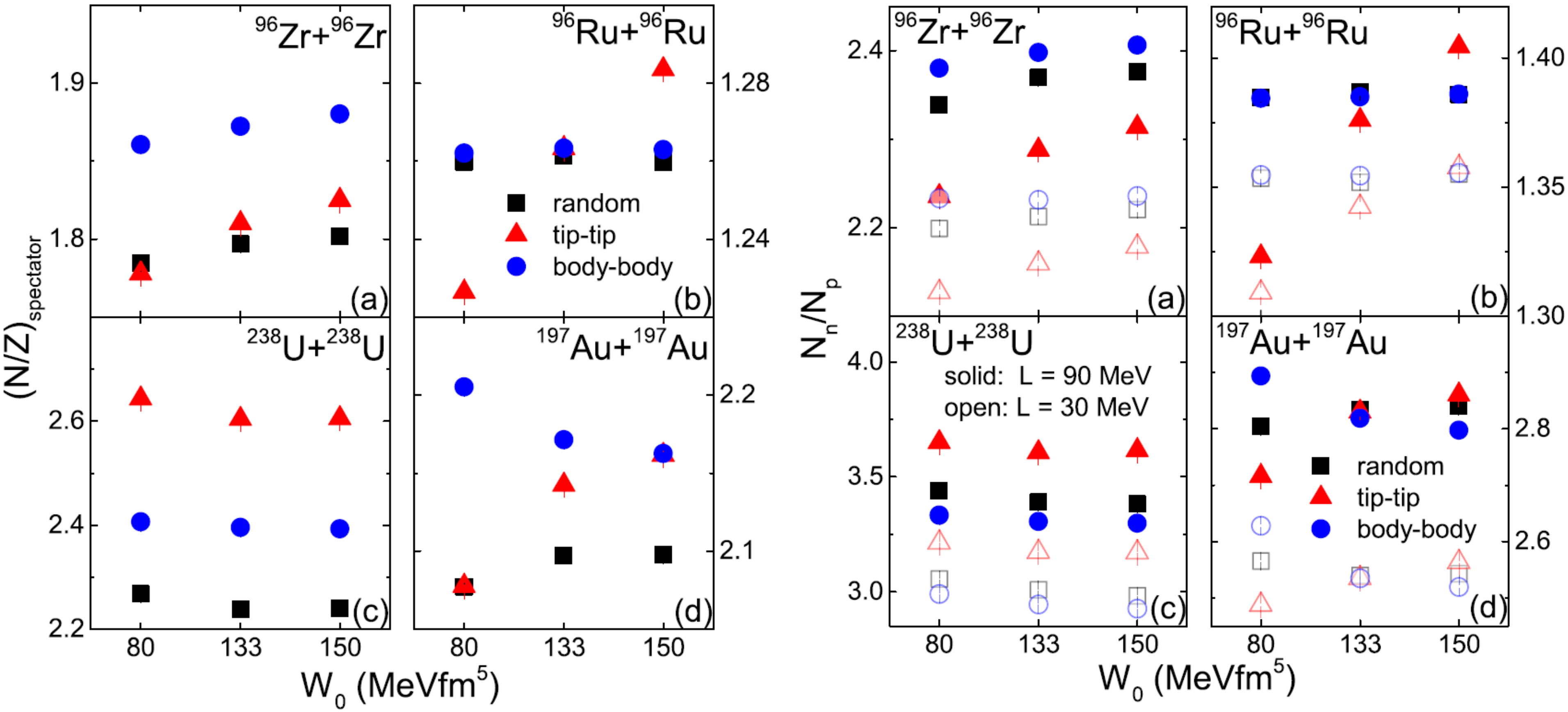

- **Isospin asymmetry increased for free spectator nucleons compared to spectator matter**
- **Comparing N_n/N_p in triggered tip-tip and body-body Ru+Ru as well as Au+Au collisions may probe $\Delta r_{np}(\theta)$ and W_0**
- **Such effect is independent of L**

α-cluster structure in light nuclei from Brink wave function

Hamiltonian $$\hat{H} = \sum_{i=1}^{A} E_i^{\mathrm{c.m.}} + \sum_{i<j} V^{NN}(r_{ij}) + \sum_{i<j} V^{\mathrm{Coul}}(r_{ij}) + \sum_{i<j} V^{ls}(r_{ij})$$

Volkov No.2 force $$V^{NN}(r_{ij}) = \left(V_1 e^{-\alpha_1 r_{ij}^2} - V_2 e^{-\alpha_2 r_{ij}^2}\right)(W - M\hat{P}_\sigma \hat{P}_\tau + B\hat{P}_\sigma - H\hat{P}_\tau)$$

spin-orbit interaction $$V^{ls}(r_{ij}) = u_{ls}\left(e^{-\alpha_3 r_{ij}^2} - e^{-\alpha_4 r_{ij}^2}\right)\vec{L}\cdot\vec{S}\hat{P}_{31}$$

$$|\Phi^{\mathrm{Brink}}\rangle = (C_\alpha^\dagger)^n |\mathrm{vac}\rangle$$

$$C_\alpha^\dagger = \int d^3r_1 \cdots d^3r_4 \; \phi(\vec{r}_1 - \vec{R}) a^\dagger_{\sigma_1,\tau_1}(\vec{r}_1) \cdots \phi(\vec{r}_4 - \vec{R}) a^\dagger_{\sigma_4,\tau_4}(\vec{r}_4)$$

^{12}C

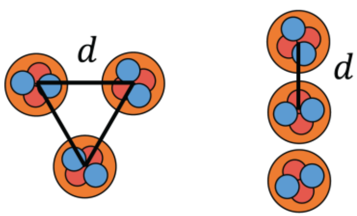

^{16}O

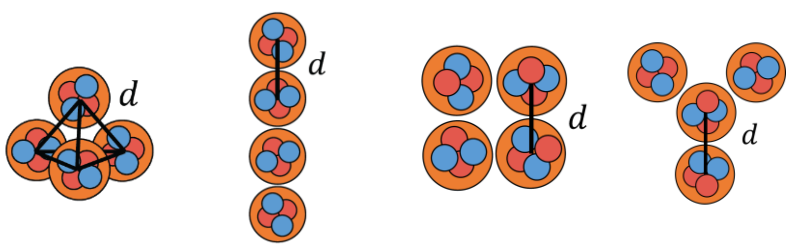

^{20}Ne

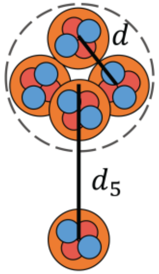

Distance parameters are determined by minimizing the energy for a particular configuration

density distribution $$\rho(\vec{a}) = \frac{\langle\Phi|\sum_{i=1}^{A}\delta(\vec{r}_i - \vec{a})|\Phi\rangle}{\langle\Phi|\Phi\rangle} = \sum_{i=1}^{A}\rho_i(\vec{a})$$

Forward/backward particle yields as a probe of α-cluster configuration in ^{12}C and ^{16}O

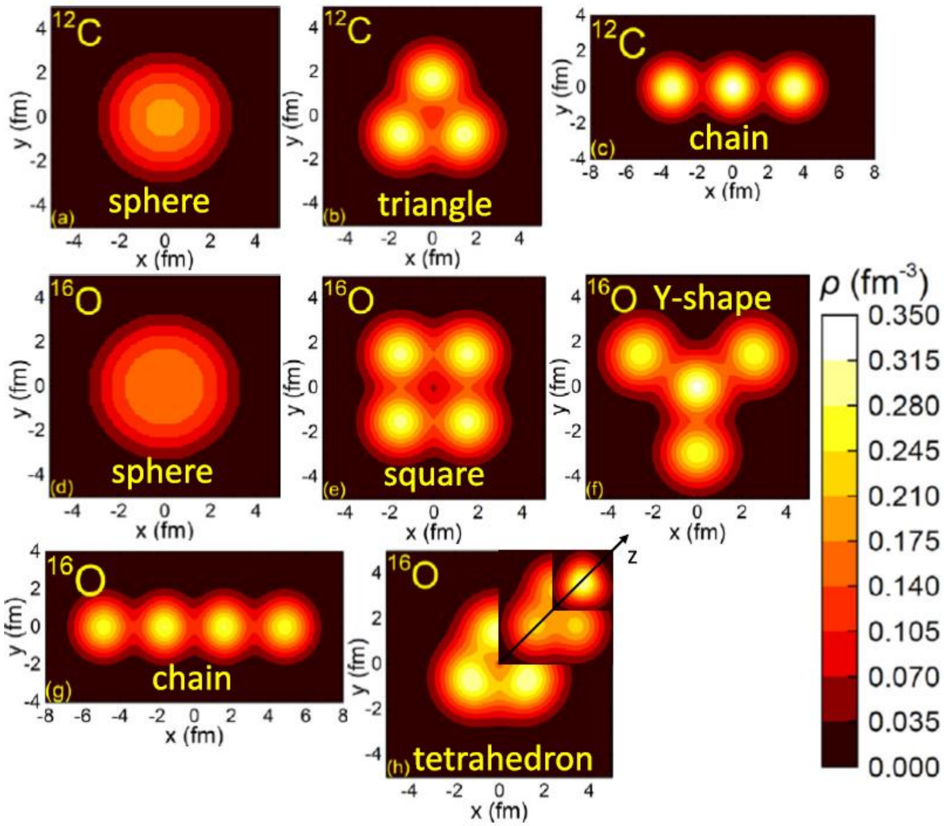

Root-mean-square (RMS) radii in fm of ^{12}C and ^{16}O for different configurations.

	sphere	triangle	square	chain	Y-shape	tetrahedron
^{12}C	2.49	2.45	-	3.29	-	-
^{16}O	2.69	-	2.77	4.06	3.09	2.45

charged-particle multiplicity distribution from AMPT

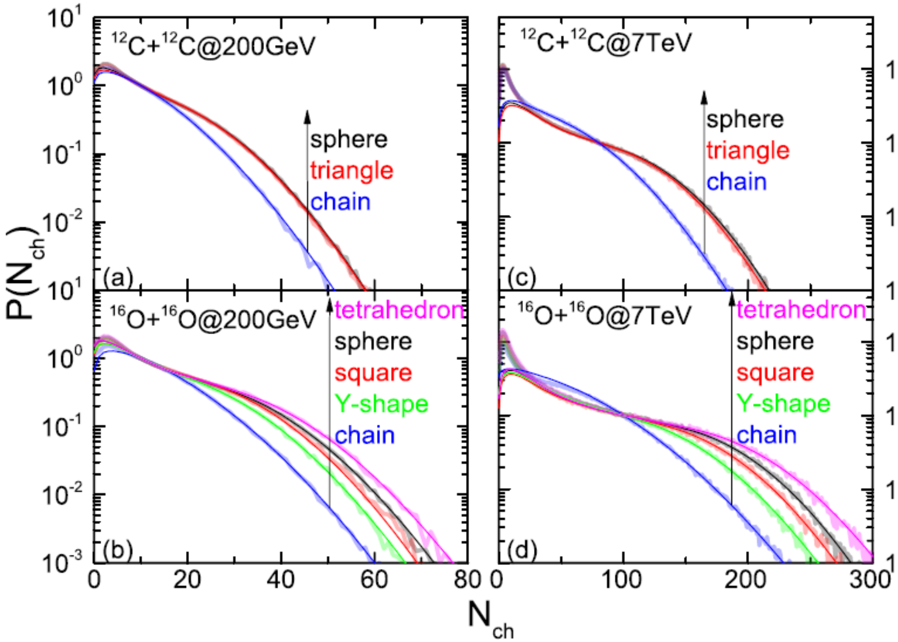

L.M. Liu, S.J. Li, Z. Wang, JX, Z.Z.Ren, and X.G. Huang, PLB (2024)

Forward/backward particle yields as a probe of α-cluster configuration in ^{12}C and ^{16}O

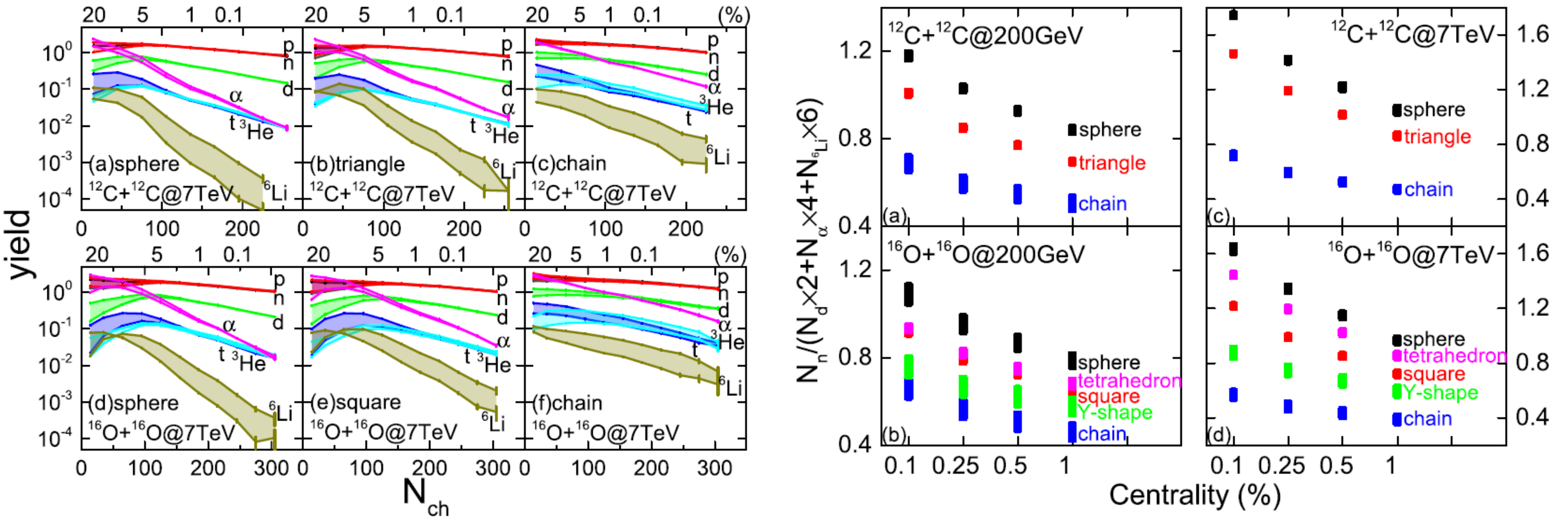

- With initially α-cluster structure, neutrons and protons are more likely to form α particles or light nuclei at forward/backward rapidities.
- Chain configuration leads to more α particles or light nuclei compared to more compact configurations.
- The uncertainties in the deexcitation process are largely reduced in ultracentral collisions.

L.M. Liu, S.J. Li, Z. Wang, JX, Z.Z.Ren, and X.G. Huang, PLB (2024)

Directly probing existence of α-cluster structure in ^{20}Ne

It is difficult to distinguish the two cases through mid-rapidity observables in ^{20}Ne+^{20}Ne collisions based on AMPT.

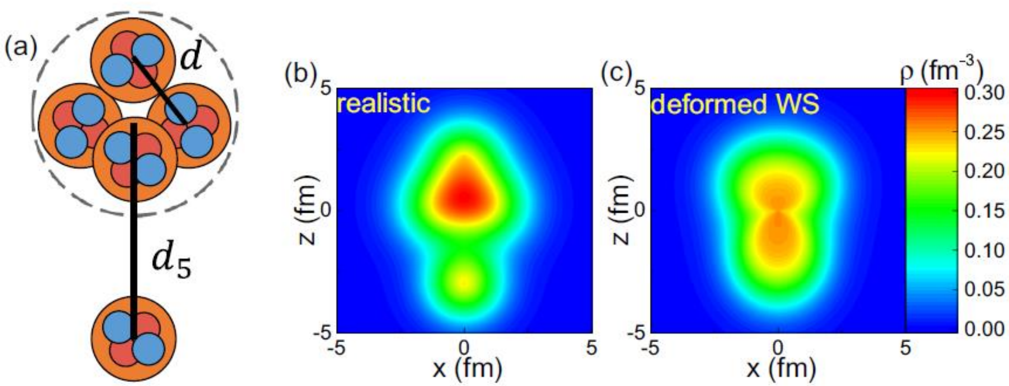

We fit the realistic density distribution with the deformed WS form, so they have the overall similar shape.

$$\rho(r,\theta) = \frac{\rho_0}{1+\exp[(r-R(\theta))/a]}$$

$$R(\theta) = R_0\left[1+\sum_{n=2,3}\beta_n Y_{n,0}(\theta)\right]$$

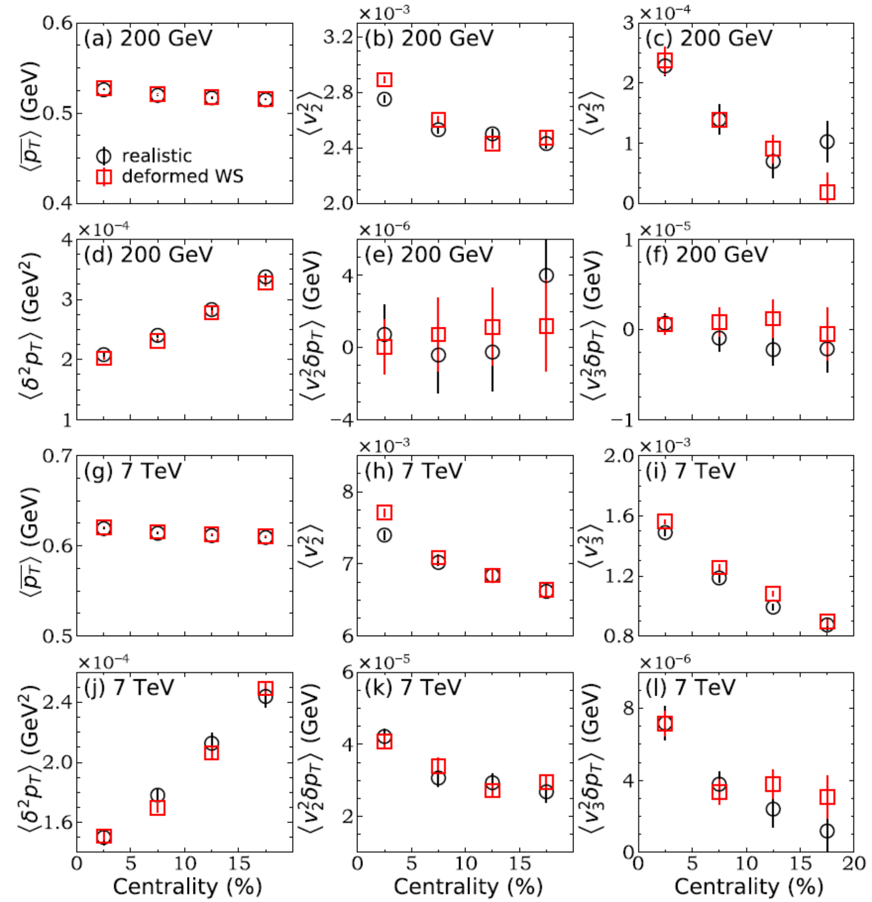

L.M. Liu, H.C. Wang, S.J. Li, C.J. Zhang, JX, Z.Z.Ren, J.Y. Jia, and X.G. Huang, PRC (2025)

Directly probing existence of α-cluster structure in ^{20}Ne

bars: with deexcitation
symbols: without deexcitation

^{20}Ne+^{20}Ne@200GeV

^{20}Ne+^{20}Ne@7TeV

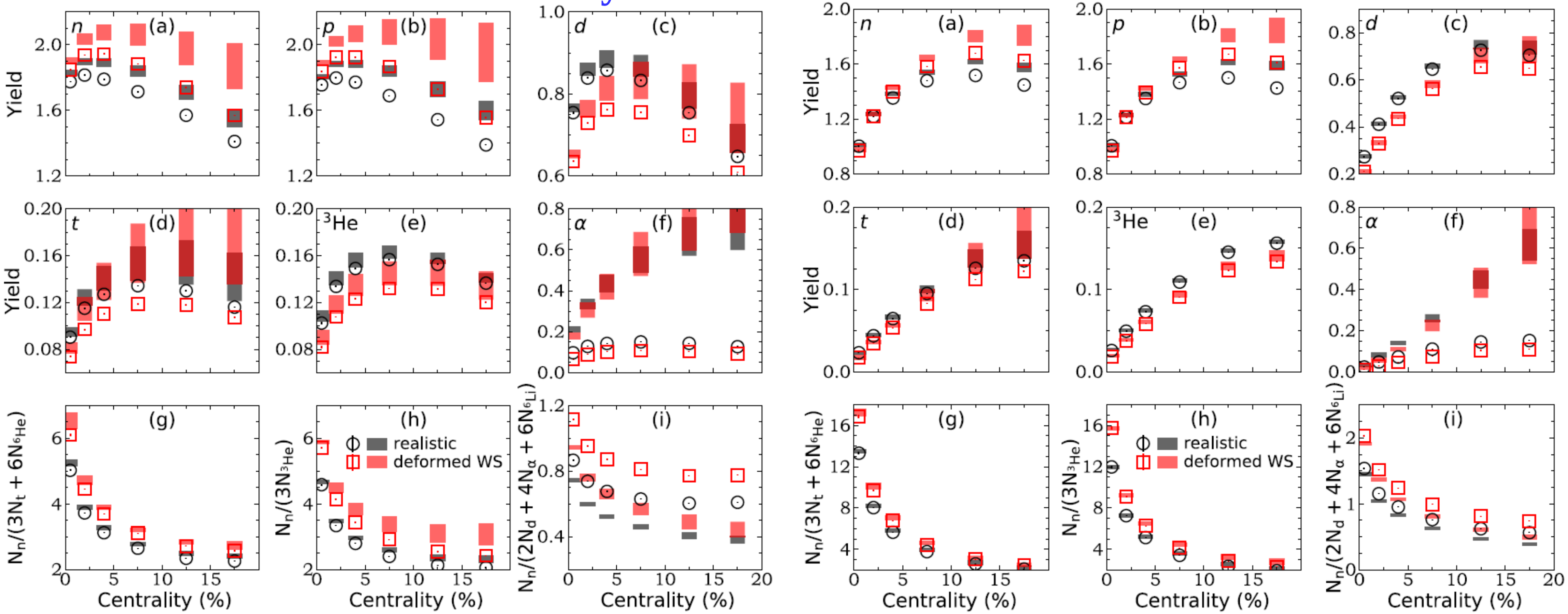

- Small spectator nucleon yield and larger yields of α particles and light nuclei are observed with initially α-cluster structure in UCC.
- Taking the yield ratio further reduces the theoretical uncertainty.
- 20% effect at RHIC and 25% effect at LHC

L.M. Liu, H.C. Wang, S.J. Li, C.J. Zhang, JX, Z.Z.Ren, J.Y. Jia, and X.G. Huang, PRC (2025)

Summary

- **Free spectator particle yield: clean probes**
- **Ultracentral HIC: free from deexcitations**
- **Probe neutron-skin thickness Δr_{np}~L**
  - $(N_n)^{Zr+Zr}/(N_n)^{Ru+Ru}$ **reduce uncertainties**
  - $(N_n/N_p)^{Zr+Zr}/(N_n/N_p)^{Ru+Ru}$ **cancel detecting efficiency**
- **Triggering collision configurations: $\Delta r_{np}(\theta)$~W_0**
- **Probe α-cluster structure/configuration in $^{16}O+^{16}O$ and $^{20}Ne+^{20}Ne$**
  - $N_n/(2N_d+4N_\alpha+6N^6{}_{Li})$
  - $N_n/(3N_t+6N^6{}_{He})$
  - $N_n/(3N^3{}_{He})$

Thank you!

junxu@tongji.edu.cn